

## Biaxial-strain effect on excitonic transitions $E_0$ and $E_0 + \Delta_0$ in the temperature range 4.5–200 K and Zeeman splitting in ZnSe/GaAs epilayers

D. Coquillat, F. Hamdani, J. P. Lascaray, O. Briot, N. Briot, and R. L. Aulombard

*Groupe d'Etude des Semiconducteurs, Université Montpellier II, Place Eugène Bataillon, 34095 Montpellier CEDEX, France*

(Received 21 May 1992; revised manuscript received 2 November 1992)

Identification of heavy-hole and light-hole excitonic transitions is made by reflectivity and magnetocircular dichroism in strained metal-organic vapor-phase-epitaxy-grown ZnSe/GaAs epilayers with a thickness range between 0.10 and 0.78  $\mu\text{m}$  at 4.5 K. The observed splitting of the exciton transitions due to the lattice mismatch is constant up to 200 K. It is explained by the very small variation ( $< 2\%$ ) of the lattice mismatch strain in this temperature range. Zeeman splitting of  $|\pm\frac{3}{2}, \pm\frac{1}{2}\rangle$  and  $|\pm\frac{1}{2}, \mp\frac{1}{2}\rangle$  transitions are measured at 5.5 T and effective  $g$  values  $g^{3/2} = -0.24$  and  $g^{1/2} = 0.57$  are determined.

### I. INTRODUCTION

The wide-band-gap zinc selenide has been, in recent years, of great interest because of its potential for use in optoelectronic devices in the short-wavelength range. Strain is created at the ZnSe/GaAs interface by the lattice mismatch and the different thermal-expansion coefficients of both compounds. Beyond the critical thickness about 0.15  $\mu\text{m}$ , a large density of dislocations, which is formed near the interface, releases the strain.<sup>1,2</sup> Concerning the growth of epitaxial thin films, numerous difficulties were identified in order to obtain  $p$ - $n$  junctions. The most important step concerns the  $p$ -type doping of ZnSe. Recently, epitaxial growth techniques such as molecular-beam epitaxy (MBE) and metal-organic vapor-phase epitaxy (MOVPE) allowed one to grow  $n$ -type materials and some progress was made in  $p$ -type fabrication of ZnSe materials. Following the successful crystal growth of Li and N  $p$ -type doped ZnSe, Haase and co-workers,<sup>3,4</sup> and afterwards Jeon *et al.*,<sup>5</sup> fabricated the first laser diodes using the MBE technique. However, as they indicated in their paper, further developments are still needed to improve the quality of materials.

In order to characterize the materials, the optical measurements, which are contactless, are now the best methods. Indeed, electrical characterization is difficult due to the lack of suitable ohmic contacts on  $p$ -type materials.<sup>6,7</sup> Optical measurements by means of various modulation techniques have been made besides conventional ones such as optical absorption and reflectivity spectra. Magnetocircular dichroism is a kind of modulation spectroscopy and has been proved to be very powerful in understanding the electronic properties of semiconductors. In a magnetic field all the degenerate bands split into subbands that have their own characteristic polarization.<sup>8–13</sup> Based on magnetocircular-dichroism measurements, we are able to determine easily the excitonic transition energy in strained epilayers. The purpose of the present work is to determine from reflectivity and magnetorefectivity measurements the energy of excitonic transitions for heavy holes,  $E_{\text{hh}}$ , and for light holes,  $E_{\text{lh}}$ , and the energy of the spin-orbit component of MOVPE-

grown ZnSe/GaAs epilayers with a thickness range between 0.10 and 0.78  $\mu\text{m}$  at liquid helium temperature. We have investigated the temperature dependence of the excitonic transitions and the temperature dependence of the mismatch splitting in the temperature range 4.5–200 K. Experimental results of Zeeman splitting for both heavy-hole and light-hole excitonic transitions using magnetocircular dichroism are obtained and the corresponding effective  $g$  values are calculated.

### II. EXPERIMENT

The growth was carried out in an ASM-France-OMR 12 MOVPE equipment. In this paper we are reporting results obtained on ZnSe layers grown using two classical procedures, i.e., the combination of alkyls or the combination of zinc alkyl and  $\text{H}_2\text{Se}$ , as sources (see Table I).

In the case of organometallic reactants (dimethylzinc: DMZn + diethylselenium: DESe), two crystal-growth methods were used. The standard procedure was used to obtain epilayers grown at temperatures about 500 °C, while the "double zone reactor" technique, previously described,<sup>14</sup> allows us to use low growth temperatures, about 300 °C. With the combination of zinc alkyl and  $\text{H}_2\text{Se}$ , the triethylamine-dimethylzinc adduct [DMZn(NEt<sub>3</sub>) supplied by EPICHEM Ltd.-Great Britain] was used to avoid prereactions.

The reflectivity of the excitonic structures was performed in a standard setup in the temperature range 4.5–300 K. Magnetorefectivity measurements were per-

TABLE I. Experimental conditions for MOVPE growth of ZnSe.

Sample	Thickness ( $\mu\text{m}$ )	Growth temperature (°C)	Reactants
ON10C	0.10	300	DMZn + DESe
ON10B	0.15	300	DMZn + DESe
ON15B	0.78	500	DMZn + DESe
BZS1H	0.369	300	DMZn(NEt <sub>3</sub> ) + H <sub>2</sub> Se
BZS1C	0.416	300	DMZn(NEt <sub>3</sub> ) + H <sub>2</sub> Se

formed in the Faraday configuration in a 5.5-T magnetic field and the magnetocircular-dichroism technique was previously described.<sup>15,16</sup> The reflectivity was measured using a chopper with a frequency of 23 Hz. At the same time the magnetocircular-dichroism signal ( $I^{\sigma^+} - I^{\sigma^-}$ ) was measured by means of a Hinds photoelastic modulator with a frequency of 50 kHz. The measurements allow one to determine absolute values of circular polarization rate  $P = (I^{\sigma^+} - I^{\sigma^-}) / (I^{\sigma^+} + I^{\sigma^-})$  and reflectivity  $R = (I^{\sigma^+} + I^{\sigma^-}) / 2$  in arbitrary units. The measurements were done typically at 1-Å intervals, with a time constant of 0.3 s.

### III. EXPERIMENTAL RESULTS AND DISCUSSION

#### A. Strain effects on $E_0$ and $E_0 + \Delta_0$ transitions

In zinc-blende-type semiconductors, in the absence of strain, the valence bands at the center of the Brillouin zone consist of a fourfold  $\Gamma_8$  multiplet ( $J = \frac{3}{2}$ ,  $m_h = \pm\frac{1}{2}, \pm\frac{3}{2}$ ) and a  $\Gamma_7$  doublet ( $J = \frac{1}{2}$ ,  $m_h = \pm\frac{1}{2}$ ). Transitions from the  $\Gamma_8$  and  $\Gamma_7$  multiplets to the  $s$ -like  $\Gamma_6$  conduction band are labeled  $E_0$  and  $E_0 + \Delta_0$ , respectively (Fig. 1). The biaxial strain splits the  $\Gamma_8$  multiplet into a heavy-hole ( $J = \frac{3}{2}$ ,  $m_h = \pm\frac{3}{2}$ ) and a light-hole ( $J = \frac{3}{2}$ ,  $m_h = \pm\frac{1}{2}$ ) subband. Here, we write the excitonic transitions as  $|m_h, m_s\rangle$  with ( $m_h = \pm\frac{3}{2}, \pm\frac{1}{2}$  and  $m_s = \pm\frac{1}{2}$  characterizing  $\Gamma_8$  valence band and  $\Gamma_6$  conduction-band states, respectively). The hydrostatic component of the strain shifts the  $\Gamma_7$  valence-band doublet relative to the  $\Gamma_6$  conduction band.

For the epilayers ZnSe/GaAs grown on (001)-oriented substrates, the strain tensors components are given by

$$\begin{aligned} \varepsilon = \varepsilon_{xx} = \varepsilon_{yy} &= \frac{a^{\parallel} - a_{\text{ZnSe}}}{a_{\text{ZnSe}}}, \\ \varepsilon_{zz} &= 2 \frac{C_{12}}{C_{11}} \varepsilon, \end{aligned} \quad (1)$$

where  $\varepsilon$  has been defined to be negative for compressive strain,  $a^{\parallel}$  is the lattice constant of the epilayer along the layer surface,  $a_{\text{ZnSe}}$  is the lattice constant of bulk, and  $C_{ij}$  are the elastic stiffness constants of the ZnSe material. In

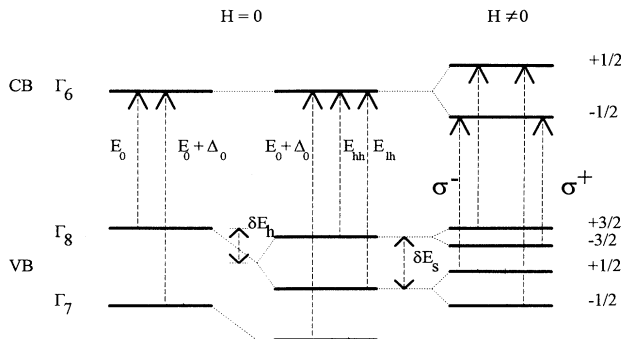


FIG. 1. A schematic representation of band splittings in a strained ZnSe/GaAs epilayer (in compression). Transitions allowed in the Faraday configuration are marked by arrows.

ZnSe/GaAs, the residual strain is not sufficient to induce coupling between the light-hole and the spin-orbit subbands ( $\delta E_s / \Delta_0 \ll 1$ ) and the energy shifts with respect to its zero stress value for excitonic transitions associated with  $\Gamma_6$ - $\Gamma_8$  and  $\Gamma_6$ - $\Gamma_7$  band extrema are thus given by

$$\Delta E_{\text{hh}} = \left[ 2a \frac{C_{11} - C_{12}}{C_{11}} - b \frac{C_{11} + 2C_{12}}{C_{11}} \right] \varepsilon = \delta E_h - \frac{1}{2} \delta E_s, \quad (2)$$

$$\Delta E_{\text{lh}} = \left[ 2a \frac{C_{11} - C_{12}}{C_{11}} + b \frac{C_{11} + 2C_{12}}{C_{11}} \right] \varepsilon = \delta E_h + \frac{1}{2} \delta E_s, \quad (3)$$

$$\Delta(E_0 + \Delta_0) = \left[ 2a \frac{C_{11} - C_{12}}{C_{11}} \right] \varepsilon = \delta E_h, \quad (4)$$

where  $a$  is the hydrostatic pressure deformation potential,  $b$  is the shear deformation potential. The energy difference  $\delta E_s$  between the heavy hole  $E_{\text{hh}}$  ( $|\pm\frac{3}{2}, \pm\frac{1}{2}\rangle$ ) and light-hole  $E_{\text{lh}}$  ( $|\pm\frac{1}{2}, \pm\frac{1}{2}\rangle$ ) excitonic transitions as well as the hydrostatic shift  $\delta E_h$  are linear in  $\varepsilon$ . Using the deformation potential given by Rockwell *et al.*<sup>17</sup> ( $a = -4.53$  eV,  $b = -1.17 \pm 0.03$  eV), lattice mismatch splitting of the  $\Gamma_8$  valence band is given by

$$\delta E_s = E_{\text{lh}} - E_{\text{hh}} = 2b \left[ \frac{C_{11} + 2C_{12}}{C_{11}} \right] \varepsilon = 5152\varepsilon \text{ (meV)}. \quad (5)$$

The value of the spin-orbit splitting can be estimated for each layer by

$$\Delta_0 = (E_0 + \Delta_0) - \frac{E_{\text{hh}} + E_{\text{lh}}}{2}. \quad (6)$$

#### B. Identification of excitonic transitions

Figure 2(a) presents the reflectivity spectra of ZnSe epilayers with different thicknesses measured at liquid helium temperature in spectral region of the ZnSe band edge. We also present in the same figure, a reflectivity spectra of bulk ZnSe grown by the Bridgman method. As we can see, the shape of the reflectivity spectrum is very different for each epilayer; identification of the excitonic transition needs detailed analysis. Concerning the reflectivity structure shape similar to ZnSe bulk, for instance, we have considered the inflexion point of each reflectivity structure as the energy of excitonic transition. In this case, to determine the inflexion-point energy accurately we have numerically derived the reflectivity spectra [Fig. 2(b)] and taken the minimum of the derivative curve as excitonic transition energy.

The spectrum of 0.15- $\mu\text{m}$ -thick epilayer is characterized by two main reflectivity structures at 2.8018 and 2.8139 eV, that we have assigned to heavy-hole ( $E_{\text{hh}}$ )  $|\pm\frac{3}{2}, \pm\frac{1}{2}\rangle$  and light-hole ( $E_{\text{lh}}$ )  $|\pm\frac{1}{2}, \pm\frac{1}{2}\rangle$  excitonic transitions. However, we note that the lower-energy structure is at a smaller energy than the free exciton of bulk ZnSe

(Table II). In order to verify whether or not this structure is a consequence of interference fringes, we have studied the reflectivity spectrum of this epilayer with an angle of incidence of  $45^\circ$ . In this case, the periodicity of fringes should be smaller due to the larger path through the layer. As can be seen in Fig. 3, the shape of the structure is not changed, contrary to the case observed for the feature at the lower-energy position visible in the  $0.369\text{-}\mu\text{m}$ -thick epilayers described later in the text. Based on this observation, the structure at  $2.8018\text{ eV}$  does not support an interference fringe interpretation. On the other hand, the intensity of the structure at the lower-energy position is about three times stronger than the one at the higher-energy position. This value is very close to the oscillator-strength ratio of heavy-hole and light-hole excitonic transitions, and is in good agreement with results of Lee *et al.*<sup>18</sup> on thin ZnSe/GaAs epilayers.

Figure 2(a) shows three quasi-identical spectra for a  $0.10\text{-}\mu\text{m}$  sample that is measured just after growth, several months, and one year after growth. The presence of three structures draws immediate attention. The lower-energy structure became weaker, and finally vanished in the course of time. The feature at  $2.7977\text{ eV}$  is attributed to a donor-bound exciton; its energy is close to

that observed at  $2.798\text{ eV}$  in bulk ZnSe by Venghaus and Lambrich<sup>19</sup> and close to the energy of peak associated with the donor-bound exciton observed in the photoluminescence spectrum of a ZnSe/GaAs layer.<sup>20</sup> No definitive interpretation of the vanishing on this reflectivity structure has been provided. The two remaining structures of Fig. 2(a) are assigned to  $E_{hh}$  and  $E_{lh}$  excitonic transitions. Due to the unexpected reflectivity spectrum, and the maxima obtained for numerically derivative spectra [minima instead for the other layers in Fig. 2(b)], no decisive conclusion could be derived to evaluate the energy of  $E_{hh}$  and  $E_{lh}$ . In order to determine these energies accurately, we have performed magnetocircular dichroism.

Following Venghaus and co-workers<sup>19,21,22</sup> and Gutowski, Presser, and Kudlek,<sup>20</sup> we will discuss our results in the case of negligible electron-hole spin exchange. In the Faraday configuration for  $B \parallel \langle 001 \rangle$  the magnetic field splits, on the one hand, the  $|\pm\frac{3}{2}, \pm\frac{1}{2}\rangle$  excitonic transition in  $|+\frac{3}{2}, +\frac{1}{2}\rangle$  and  $|-\frac{3}{2}, -\frac{1}{2}\rangle$  transitions with equal oscillator strength observable in  $\sigma^-$  circular polarization ( $\Delta m = -1$ ) and  $\sigma^+$  polarization ( $\Delta m = +1$ ), respectively, and on the other hand, the  $|\pm\frac{1}{2}, \mp\frac{1}{2}\rangle$  excitonic transition in two transitions  $|+\frac{1}{2}, -\frac{1}{2}\rangle$  and  $|-\frac{1}{2}, +\frac{1}{2}\rangle$  polar-

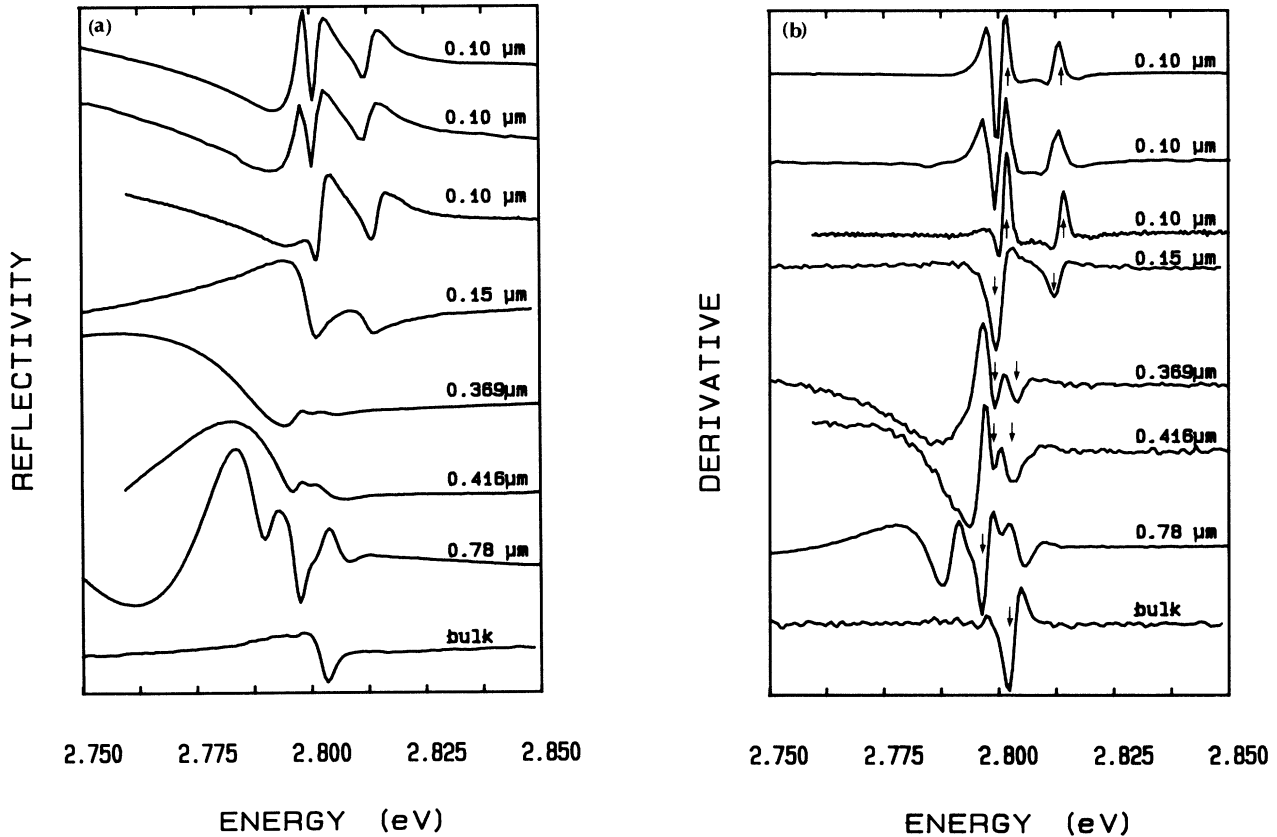


FIG. 2. (a) Reflectivity spectra of ZnSe/GaAs epilayers with thickness range between  $0.10$  and  $0.78\text{ }\mu\text{m}$  and for bulk ZnSe at  $T=4.5\text{ K}$ . (b) Numerical derivative of reflectivity spectra. The first spectrum for the  $0.10\text{-}\mu\text{m}$  sample (top) is measured just after growth. The second is measured several months and the third one year after growth. Excitonic transitions  $E_{hh}$  and  $E_{lh}$  are indicated by arrows.

TABLE II. Energies at 4.5 K of  $E_0$ , heavy-hole  $E_{hh}$ , light-hole  $E_{lh}$ , and  $E_0 + \Delta_0$  excitonic transitions of ZnSe epilayers grown on GaAs (100) as a function of the layer thickness.  $\delta E_s = E_{lh} - E_{hh}$  is the splitting due to the lattice mismatch, and  $\Delta_0$  the value of the spin-orbit interaction.

Thickness ( $\mu\text{m}$ )	$E_0$ (eV)	$E_{hh}$ (eV)	$E_{lh}$ (eV)	$\delta E_s$ (meV)	$E_0 + \Delta_0$ (eV)	$\Delta_0$ (meV)
0.10		2.8018 <sup>a</sup>	2.8139 <sup>a</sup>	12.1	3.2376 <sup>a</sup>	429
			2.8017 <sup>b</sup>	2.8138 <sup>b</sup>		
0.15		2.7994 <sup>a</sup>	2.8121 <sup>a</sup>	12.6	3.2287 <sup>a</sup>	423
0.369		2.79920 <sup>a</sup>	2.8040 <sup>a</sup>	4.8	3.2228 <sup>a</sup>	421
			2.79925 <sup>b</sup>			
0.416		2.7991 <sup>a</sup>	2.8029 <sup>a</sup>	3.8	3.2233 <sup>a</sup>	422
			2.7994 <sup>b</sup>			
0.78		2.7965 <sup>a</sup>				
Bulk	2.8024 <sup>a</sup>				3.2235 <sup>a</sup>	421

<sup>a</sup>Estimated from numerical derivative of reflectivity.

<sup>b</sup>Estimated from magnetocircular dichroism.

ized in  $\sigma^-$  and  $\sigma^+$  polarization, respectively (Fig. 1). The Zeeman splittings may be written as

$$\Delta E^{3/2} = |-\frac{3}{2}, -\frac{1}{2}\rangle - |+\frac{3}{2}, +\frac{1}{2}\rangle,$$

$$\Delta E^{1/2} = |-\frac{1}{2}, +\frac{1}{2}\rangle - |+\frac{1}{2}, -\frac{1}{2}\rangle.$$

They turn out to be small compared to the line width of the reflectivity structure and no clear difference can be observed between the two  $\sigma^+$  and  $\sigma^-$  reflectivity spectra. For this reason, the sum and the difference (called magnetocircular dichroism) of the  $\sigma^+$  and  $\sigma^-$  polarized reflectivity are measured. The circular polarization spectra  $P = (I^{\sigma^+} - I^{\sigma^-}) / (I^{\sigma^+} + I^{\sigma^-})$  is measured and presents sharp peaks at the energy of excitonic transitions

(see Fig. 4). The observed  $P$  negative (positive) values in the region of heavy (light) excitonic transitions indicate that the values of Zeeman splitting  $\Delta E^{3/2}$  and  $\Delta E^{1/2}$  are opposite in sign. Calculations of Zeeman splittings are discussed later in the text. Neglecting the diamagnetic shift ( $\leq 0.25$  meV at 5.5 T for  $\sigma$  components in bulk ZnSe crystal after Venghaus and co-workers<sup>19,21,22</sup>) the minima at 2.8018 eV and the maxima at 2.8139 eV correspond to the energy of heavy-hole states and light-hole states, respectively in the absence of a magnetic field. It is interesting to note from Table II the quite similar energy values of extrema obtained from both the numerically derivated reflectivity spectrum and the polarization spectrum. The splitting of excitonic transitions due to the lat-

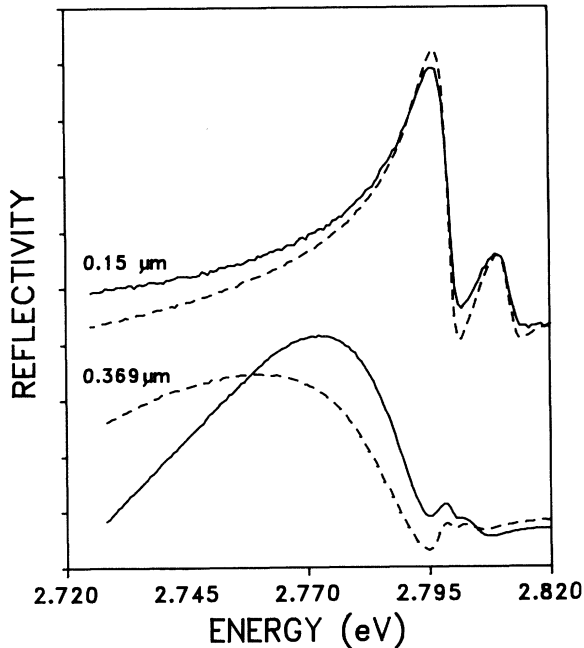


FIG. 3. Reflectivity spectra with angle of incidence to the normal of the face of the epilayer being 90° (dashed line) and 45° (solid line) at 4.5 K for two different layer thicknesses (0.15 and 0.369  $\mu\text{m}$ ).

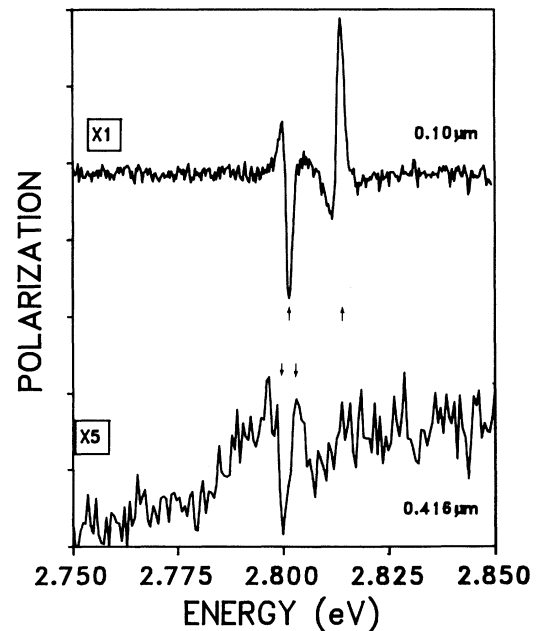


FIG. 4. Circular polarization spectra  $P = (I^{\sigma^+} - I^{\sigma^-}) / (I^{\sigma^+} + I^{\sigma^-})$  exhibit excitonic transitions  $E_{hh}$  and  $E_{lh}$  at  $T = 4.5$  K and in a 5.5-T magnetic field for two different layer thicknesses.

tice mismatch of the 0.10- $\mu\text{m}$ -thick ZnSe epilayer is  $\delta E_s = 12.1$  meV.

The strain in the ZnSe epilayers is expected to decrease as the thickness of the layer increases to about 1  $\mu\text{m}$ . Figure 2(a) shows the reflectivity spectra of 0.369- and 0.416- $\mu\text{m}$ -thick ZnSe epilayers. A combination of the normal and 45° reflectivity measurements allows us to associate the feature between 2.75 and 2.79 eV with interference fringes (Fig. 3). Additional evidence in support of this assertion is provided by observation of magnetocircular dichroism (Fig. 4). No structure is revealed in the polarization spectra for these two epilayers in this range of energy (see, for example, the 0.416- $\mu\text{m}$ -thick epilayer). However, to maximum and minimum values indicated by arrows on polarization spectra correspond two minima in the numerically derivative reflectivity spectra [see Fig. 2(b) and Table II]. These extrema could then be alternatively attributed to the excitonic transitions associated with  $E_{hh}$  and  $E_{lh}$ , respectively. The transition energies and the lattice mismatch splitting  $\delta E_s$  obtained from the above analysis are listed in Table II.

Figure 5 shows the  $E_0 + \Delta_0$  reflectivity spectra obtained at  $T = 4.5$  K for different thicknesses of the epilayers. These transitions are very weak, so that the associated structure is only visible for good crystallized material. The energy of the transition is taken as the inflexion point of the structure determined from the numerically derivative curve. Values are given in Table II. The energy of the  $E_0 + \Delta_0$  structure decreases as the thickness increases from 0.10 to 0.78  $\mu\text{m}$ , until reaching a value very close to that of  $E_0 + \Delta_0$  for an unstrained ZnSe crystal.<sup>23</sup> These values are in good agreement with results on ZnSe/GaAs obtained by Stoehr *et al.*<sup>24</sup> On account of the single structure in this range of energy, unambiguous identification is possible for the  $E_0 + \Delta_0$

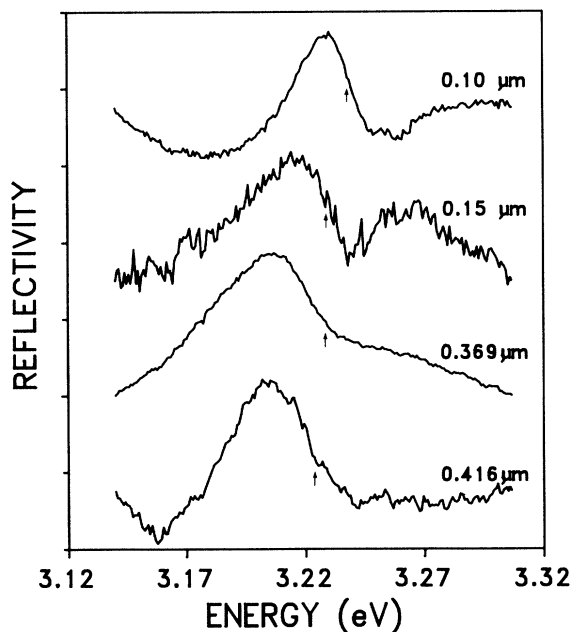


FIG. 5. Reflectivity structure associated with the  $E_0 + \Delta_0$  transition for different thicknesses of the epilayers at  $T = 4.5$  K.

transition. Consequently, the measured shift of the  $E_0 + \Delta_0$  transition of a strained layer compared with that of an unstrained crystal provides the possibility of determining easily the character (compressive or tensile) of the strain in an epilayer. The values of spin-orbit splitting determined from Eq. (6) are listed in Table II.

### C. Temperature dependence of excitonic transitions

Epitaxial growth of a thin film on a thick substrate induces a residual strain in the epilayer not only because of the lattice mismatch at the growth temperature, but also as a result of the difference of the thermal expansion coefficients. The strain and then the splitting of the fundamental excitonic transition will be dependent on the temperature of measurement, which ranged from 4.5 K to room temperature in this investigation. Figures 6 and 7 show the reflectivity spectra, respectively, in the energy range of the  $E_0$  and  $E_0 + \Delta_0$  transitions at different temperatures for the pseudomorphic 0.15- $\mu\text{m}$ -thick epilayer. The splitting between the light-hole and heavy-hole transitions, located by following the evolution of spectrum with increasing temperature, is measurable in the two thinner layers up to 175 K. For temperatures up to 200 K, the excitonic transitions become rather broad and we could not resolve the light-hole component. The energies of  $E_{hh}$ ,  $E_{lh}$ , and  $E_0 + \Delta_0$  transitions for 0.10- $\mu\text{m}$ - and 0.15- $\mu\text{m}$ -thick ZnSe layers up to room temperature have the same temperature dependence. They run parallel to each other, shifted by about 12.1 meV for the 0.10- $\mu\text{m}$ -thick epilayer and about 12.6 meV for the 0.15- $\mu\text{m}$ -thick epilayer. Data are fitted with the Varshni's empirical relation:

$$E(T) = E(0) - \frac{\alpha T^2}{T + \beta} \quad (7)$$

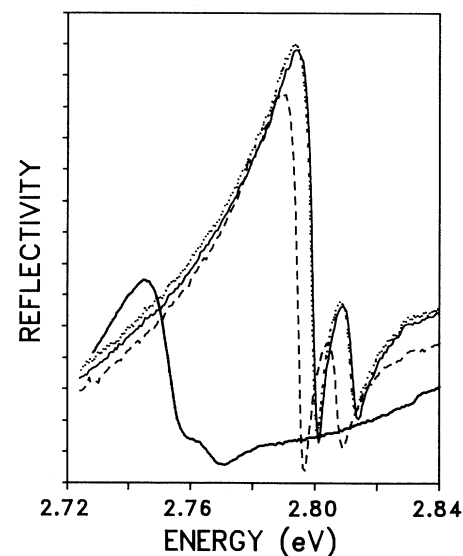


FIG. 6. Temperature dependence of the  $E_{hh}$  and  $E_{lh}$  reflectivity structure of the 0.15- $\mu\text{m}$ -thick epilayer at 4.5 K (solid curve), 19 K (dotted curve), 52 K (dashed curve), and 172 K (heavy solid curve).

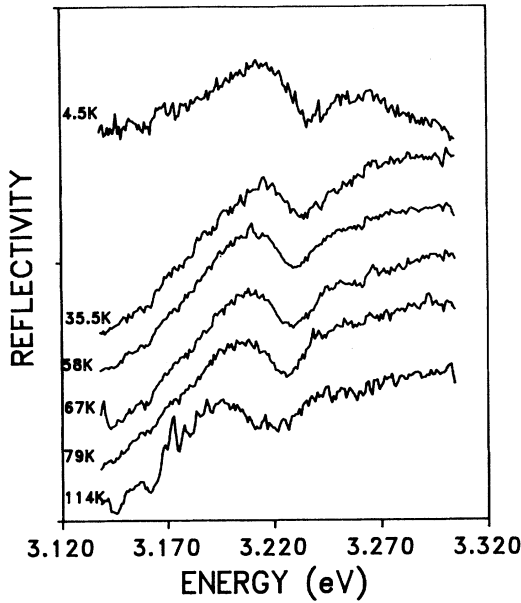


FIG. 7. Temperature dependence of the  $E_0 + \Delta_0$  reflectivity structure for 0.15- $\mu\text{m}$ -thick epilayer.

The values of fitting parameters used in Eq. (7) for the transitions  $E_{hh}$ ,  $E_{lh}$ , and  $E_0 + \Delta_0$  are  $\alpha = 8.10^{-4} \text{ eV K}^{-1}$  and  $\beta = 370 \text{ K}$ . Figure 8 displays the values of the mismatch splitting  $\delta E_s$  as a function of temperature. This is in contrast with the behavior of  $\delta E_s$ , observed by Rockwell *et al.*<sup>17</sup>

For pseudomorphic epilayers, the stress is entirely due to the lattice mismatch, and the splitting  $\delta E_s$  according to Eqs. (2) and (3) is proportional to the strain  $\epsilon_m$  given by

$$\epsilon_m = \frac{a_{\text{GaAs}} - a_{\text{ZnSe}}}{a_{\text{ZnSe}}}, \quad (8)$$

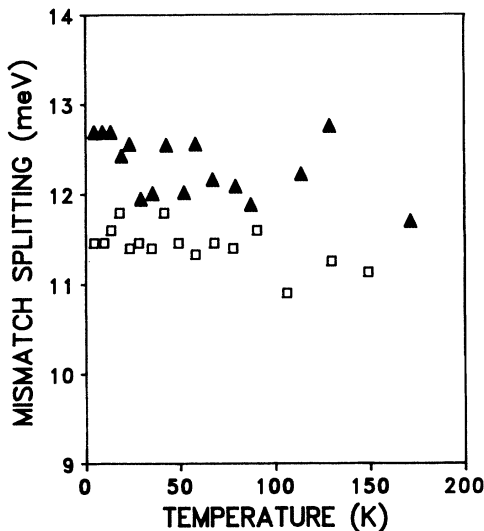


FIG. 8. Heavy-hole–light-hole splitting due to the lattice mismatch vs temperature for 0.10  $\mu\text{m}$  (open square) and 0.15  $\mu\text{m}$  (filled triangle)-thick ZnSe/GaAs epilayers.

where  $a_{\text{GaAs}}$  and  $a_{\text{ZnSe}}$  depend on the thermal-expansion coefficient when temperature is varying. It is known that there is a large difference in the thermal-expansion coefficient between ZnSe<sup>25–27</sup> and GaAs.<sup>26</sup> We have calculated the lattice parameter of GaAs and bulk ZnSe as a function of temperature from the values of the coefficient of thermal expansion and using the lattice parameters measured at room temperature  $a = 5.6692 \text{ \AA}$  for bulk ZnSe (Ref. 25) and  $a = 5.6533 \text{ \AA}$  for GaAs.<sup>28</sup> Then we have deduced the temperature dependence of the elastic strain  $\epsilon_m$  induced by the lattice mismatch calculated from Eq. (8). The variation of  $\epsilon_m$  presented in Fig. 9 is independent of the growth technique used and of the substrate temperature during growth. As can be seen, the variation of lattice mismatch strain is very small,  $\epsilon_m$  varies from  $-2.6 \times 10^{-3}$  to  $-2.65 \times 10^{-3}$  when temperature is increasing from 4.2 to 200 K, assuming that the elastic stiffness constant does not vary in this range of temperature. Consequently, at a temperature of 200 K, the mismatch splitting  $\delta E_s$  increases by only 0.26 meV over the value obtained at 4.2 K; this small variation explains the constant value of experimental  $\delta E_s$  observed on pseudomorphic epilayers in this range of temperature. Rockwell *et al.*<sup>17</sup> have reported an increase in  $\delta E_s$  of 4 meV, with increasing the temperature from 80 to 200 K; this amount of splitting variation cannot be related to the temperature variation of strain in the epilayer.

The temperature dependence of a 14- $\mu\text{m}$ -thick epilayer in tension stress<sup>29</sup> can be expressed with the same parameters as for pseudomorphic layers. In spite of the difference in the thermal-expansion coefficient for each material between 4.2 and 300 K, the same temperature

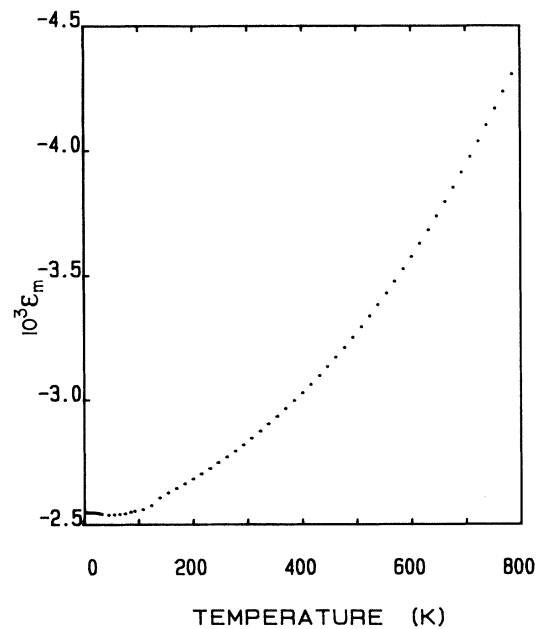


FIG. 9. Strain due to the lattice mismatch in the case of pseudomorphic epilayers ( $a_{\text{ZnSe}}$  along the layer surface is equal to  $a_{\text{GaAs}}$ ) vs temperature using the thermal-expansion coefficient given in Refs. 25–27.

dependence for pseudomorphic ZnSe/GaAs and thick ZnSe/GaAs suggests that the term containing the contribution of thermal expansion<sup>30</sup> plays no significant role in the gap variation of the ZnSe/GaAs epilayer. Our fits indicate that  $E_0$  and  $E_0 + \Delta_0$  transitions have a similar temperature dependence. This feature reflects the fact that due to its intra-atomic nature, the spin-orbit splitting should be independent of temperature.

**D. Zeeman splitting of  $|\pm\frac{3}{2}, \pm\frac{1}{2}\rangle$  and  $|\pm\frac{1}{2}, \mp\frac{1}{2}\rangle$  transitions in the Faraday configuration**

Magneto-optical experiments on free-exciton states in bulk ZnSe have been reported in magnetic fields up to 18 T by Venghaus and Lambrich<sup>19,21,22</sup> and up to 9 T by Feierabend and Weber.<sup>31</sup> Fundamental parameters such as the electron and hole effective  $g$  values, the effective mass, and the electron-hole spin-exchange energy have been derived from the diamagnetic shift and the Zeeman splitting of substates emerging from the  $E_0$  transition. In the case of bulk ZnSe, the valence band  $\Gamma_8$  is fourthly degenerate in the absence of a magnetic field. Even in a magnetic field of 18 T energy differences between the transitions are very small compared to the linewidth of the reflectivity structure and only the two predominant transitions  $|+\frac{3}{2}, +\frac{1}{2}\rangle$  and  $|-\frac{3}{2}, -\frac{1}{2}\rangle$  are easily observed. The weak  $|+\frac{1}{2}, -\frac{1}{2}\rangle$  transition is visible in magnetic fields higher than 12 T and the weak  $|-\frac{1}{2}, +\frac{1}{2}\rangle$  transition could not be observed experimentally. In pseudomorphic epilayers the situation is different. The Zeeman splitting pattern of energy bands in strained epilayers is divided, and Zeeman splitting of the two transitions associated with heavy holes and those of the two transitions associated with light holes can be treated independently with a well-adapted intensity ratio of oscillator strength.

Figure 4 shows polarization spectra for 0.10- and 0.416- $\mu\text{m}$ -thick epilayers. As we have already discussed, the energy separation  $\Delta E^{3/2}$  associated with transitions from heavy-hole states is of a sign opposite to the energy separation  $\Delta E^{1/2}$  associated with transitions from light-hole states and, consequently, effective  $g$  values have opposite signs. In the energy range of  $E_{\text{hh}}$  and  $E_{\text{lh}}$  transitions, the derivative  $d \ln R / dE$  curves were obtained and compared with the corresponding polarization spectra. In the case of pseudomorphic epilayers where the energy difference  $\delta E_s$  is sufficiently large it was found similarly to Refs. 15 and 16 that the polarization spectra repro-

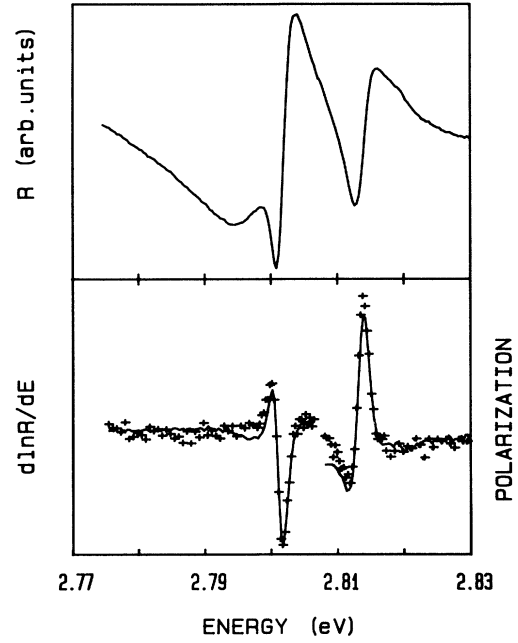


FIG. 10. Reflectivity spectrum (top) and its logarithmic derivative (continuous line, bottom) compared with polarization spectra (+ + +) for the 0.10- $\mu\text{m}$ -thick epilayer at  $T=4.5$  K and  $H=5.5$  T. Scales of  $d \ln R / dE$  and of the polarization have been chosen to obtain the best fit of the two curves.

duced quite well the form of the logarithmic derivative of the reflectivity. The results concerning the 0.10- $\mu\text{m}$ -thick epilayer are displayed in Fig. 10 for  $|\pm\frac{3}{2}, \pm\frac{1}{2}\rangle$  then  $|\pm\frac{1}{2}, \mp\frac{1}{2}\rangle$  transitions. This shows, as expected, that the magnetic field splits the excitonic transition into two components of equal magnitude observed in  $\sigma^+$  and  $\sigma^-$  circular polarization, respectively, without changing the form of the spectrum. The Zeeman splitting may be determined from the following expression:

$$P = \frac{I^{\sigma^+} - I^{\sigma^-}}{I^{\sigma^+} + I^{\sigma^-}} = \frac{\Delta R}{2R} = \frac{1}{2} \Delta E \frac{d \ln R}{dE} \quad (9)$$

Calculated values of  $\Delta E^{3/2}$  and  $\Delta E^{1/2}$  are listed in Table III. The corresponding effective  $g$  values  $g^{3/2}$  and  $g^{1/2}$  are calculated by the formula  $\Delta E = g \mu_B H$ , where  $\mu_B$  is the Bohr magneton and  $H$  is the magnetic field. The obtained effective  $g$  values are presented in Table III.

TABLE III. Zeeman splittings,  $g$  values determined from allowed transitions in the Faraday and Voigt configurations.

States	ZnSe epilayer (this paper)		Free exciton ZnSe bulk crystal Venghaus (Ref. 21)	ZnSe bulk crystal Feierabend and Weber (Ref. 31)	Donor-bound exciton ZnSe epilayer Kudlek <i>et al.</i> (Ref. 32)
	$\Delta E$ (meV) at $H=5.5$ T	$g_{\text{eff}}$	$g_{\text{eff}}$	$g_{\text{eff}}$	$g_{\text{eff}}$
$ \pm 3/2, \pm 1/2\rangle$	$\Delta E^{3/2} = -0.077$	$g_{\sigma}^{3/2} = -0.24$	$g_{\sigma,100}^{3/2} = -0.13 \pm 0.08$ $g_{\sigma,110}^{3/2} = -0.08 \pm 0.08$	$g_{\text{eff}} = 0.28 \pm 0.04$	$g_{\sigma}^{3/2}(D^0X) = 0.15 \pm 0.20$
$ \pm 1/2, \mp 1/2\rangle$	$\Delta E^{1/2} = +0.18$	$g_{\sigma}^{1/2} = +0.57$			$g_{\sigma}^{1/2}(D^0X) = 1.42 \pm 0.20$
$ \pm 1/2, \pm 1/2\rangle$			$g_{\pi}^{1/2} = 0.95 \pm 0.20$		

It is interesting to discuss these results and compare them with the exciton Zeeman splitting in bulk ZnSe crystals. Venghaus has determined the electron and hole effective  $g$  values for the case of negligible electron-hole spin-exchange energy compared to the linear Zeeman splitting ( $2\Delta_1 < 0.1$  meV). Values of  $g_{\sigma}^{3/2}$  in the Faraday configuration and  $g_{\pi}^{1/2}$  in the Voigt are reported in Table III. Feierabend and Weber<sup>31</sup> have obtained in bulk ZnSe an average value of effective  $g$  value by measuring an overall splitting between the  $\sigma^+$  and  $\sigma^-$  spectra by means of magnetocircular dichroism; results are reported in Table III.

Kudlek *et al.*<sup>32</sup> have investigated the luminescence of the  $I_2$  emission line related to neutral-donor-exciton complex ( $D^0X$ ) in magnetic field up to 15 T for ZnSe/GaAs epilayers. Our results are in agreement with the sign of the Zeeman splittings  $\Delta E_{D^0x}^{3/2}$  and  $\Delta E_{D^0x}^{1/2}$  obtained by these authors (see Fig. 3 in Ref. 20). However the ratio  $g^{1/2}/g^{3/2}$  is different in magnitude (see Table III). This could be attributed to observed  $g$  values larger for the

donor than for the free electron.<sup>33</sup>

In summary, we have used magnetocircular-dichroism measurements to study excitonic transitions in strained ZnSe/GaAs epilayers. Such a technique is powerful not only for identifying the heavy- and light-hole transitions, but also to determine Zeeman splitting and the related  $g$  factor. The measurements in the temperature range 4.5–200 K reveal that strained ZnSe/GaAs epilayers present the same temperature dependence for  $E_{hh}$ ,  $E_{lh}$ , and  $E_0 + \Delta_0$  transitions.

#### ACKNOWLEDGMENTS

The authors wish to express their thanks to R. Triboulet for bulk ZnSe material and the "Conseil Régional Languedoc-Roussillon" for supporting part of this work (MOVPE crystal growth). Groupe d'Etude des Semiconducteurs is "Unité de Recherche Associée No. 357 du Centre National de la Recherche Scientifique."

- 
- <sup>1</sup>T. Yao, Y. Okada, S. Matsui, K. Ishida, and I. Fujimoto, *J. Cryst. Growth* **81**, 518 (1987).
- <sup>2</sup>R. L. Aulombard, M. Averous, O. Briot, J. Calas, D. Coquillat, F. Hamdani, J. P. Lascaray, N. Moulin, and N. Tempier, *J. Cryst. Growth* **204**, 667 (1990).
- <sup>3</sup>R. M. Park, M. B. Troffer, C. M. Rouleau, J. M. Depuydt, and M. A. Haase, *Appl. Phys. Lett.* **57**, 2127 (1990).
- <sup>4</sup>M. A. Haase, J. Qiu, J. M. de Puydt, and H. Cheng, *Appl. Phys. Lett.* **59**, 1272 (1991).
- <sup>5</sup>H. Jeon, J. Ding, W. Patterson, A. V. Nurmikko, W. Xie, D. C. Grillo, M. Kobayashi, and R. L. Gunshor, *Appl. Phys. Lett.* **59**, 3619 (1991).
- <sup>6</sup>H. H. Farrell, M. C. Tamargo, T. J. Gmitter, A. L. Weaver, and D. E. Aspnes, *J. Appl. Phys.* **70**, 1033 (1991).
- <sup>7</sup>R. M. Park, M. B. Troffer, E. Yablonovitch, and T. J. Gmitter, *Appl. Phys. Lett.* **59**, 1896 (1991).
- <sup>8</sup>P. J. Stephens, *J. Chem. Phys.* **52**, 3489 (1970).
- <sup>9</sup>M. Altarelli and N. O. Lipari, *Phys. Rev. B* **7**, 3798 (1973).
- <sup>10</sup>K. Cho, *Phys. Rev. B* **11**, 1512 (1975).
- <sup>11</sup>M. Altarelli and N. O. Lipari, *Phys. Rev. B* **9**, 1733 (1974).
- <sup>12</sup>K. Cho, S. Suga, W. Dreybrodt, and F. Willmann, *Phys. Rev. B* **11**, 1512 (1975).
- <sup>13</sup>W. Dreybrodt, K. Cho, S. Suga, F. Willmann, and Y. Niji, *Phys. Rev. B* **21**, 4692 (1980).
- <sup>14</sup>O. Briot, R. Delmas, N. Tempier, R. Sauvezon, and R. L. Aulombard, *J. Cryst. Growth* **98**, 857 (1989).
- <sup>15</sup>J. Ginter, J. A. Gaj, and Le Si Dang, *Solid State Commun.* **48**, 849 (1983).
- <sup>16</sup>D. Coquillat, J. P. Lascaray, J. A. Gaj, J. Deportes, J. K. Furdyna, *Phys. Rev. B* **39**, 10088 (1989).
- <sup>17</sup>B. Rockwell, H. R. Chandrasekhar, M. Chandrasekhar, A. K. Ramdas, M. Kobayashi, and R. L. Gunshor, *Phys. Rev. B* **44**, 11307 (1991).
- <sup>18</sup>Y. R. Lee, A. K. Ramdas, L. A. Kolodziejski, and R. L. Gunshor, *Phys. Rev. B* **38**, 13143 (1988).
- <sup>19</sup>H. Venghaus and R. Lambrich, *Solid State Commun.* **25**, 109 (1978).
- <sup>20</sup>J. Gutowski, N. Presser, and G. Kudlek, *Phys. Status Solidi A* **120**, 11 (1990).
- <sup>21</sup>H. Venghaus, *Solid State Commun.* **26**, 199 (1978).
- <sup>22</sup>H. Venghaus, *Phys. Rev. B* **19**, 3071 (1979).
- <sup>23</sup>S. Adachi and T. Taguchi, *Phys. Rev. B* **43**, 9569 (1991).
- <sup>24</sup>M. Stoehr, F. Hamdani, J. P. Lascaray, and M. Maurin, *Phys. Rev. B* **44**, 8912 (1991).
- <sup>25</sup>H. P. Singh and B. Dayal, *Phys. Status Solidi* **23**, K93 (1967).
- <sup>26</sup>T. F. Smith and G. K. White, *J. Phys. C* **8**, 2031 (1975).
- <sup>27</sup>T. Soma, *Solid State Commun.* **34**, 927 (1980).
- <sup>28</sup>K. Mohammed, D. A. Cammack, R. Dalby, P. Newbury, B. L. Greenberg, J. Petruzello, and R. N. Bhargava, *Appl. Phys. Lett.* **50**, 37 (1987).
- <sup>29</sup>M. Stoehr, thesis, Université Montpellier, Montpellier, 1991.
- <sup>30</sup>P. B. Allen and M. Cardona, *Phys. Rev. B* **23**, 1495 (1981).
- <sup>31</sup>Feierabend and H. G. Weber, *Solid State Commun.* **26**, 191 (1978).
- <sup>32</sup>G. Kudlek, N. Presser, J. Gutowski, S. Durbin, D. Menke, M. Kobayashi, and R. L. Gunshor, *J. Cryst. Growth* **101**, 667 (1990).
- <sup>33</sup>D. M. Hofmann, B. K. Meyer, U. Probst, and K. W. Benz, *J. Cryst. Growth* **101**, 536 (1990).